

## ANALYSIS AND MEASUREMENT OF HARD HORN FEEDS FOR THE EXCITATION OF QUASI-OPTICAL AMPLIFIERS

Maha A. Ali, Sean Ortiz, Toni Ivanov and Amir Mortazawi

Department of Electrical and Computer Engineering  
University of Central Florida  
Orlando, FL 23816-2450

### ABSTRACT

Measurement and analysis of hard horn feeds for excitation of quasi-optical amplifiers has been performed. A computer program based on the mode matching technique has been developed in order to determine the aperture field distribution for pyramidal hard horns. This program can be used to optimize a hard horn's field distribution and bandwidth. Simulation and measurement results for a 31 GHz hard horn feed are presented.

### INTRODUCTION

The power produced from millimeter-wave solid-state devices drops drastically as their frequency of operation increases. Furthermore most system applications require much more power than is available or expected from a single solid-state device. This problem can be alleviated by combining the power produced from many solid-state devices. Conventional power combining techniques are inefficient at millimeter-wave frequencies, specifically when many devices are power combined. Spatial or quasi-optical power combining has shown the potential to efficiently power combine hundreds of solid-state devices and thus provide a solution to the attainment of high power at mm-wave frequencies.

The first type of quasi-optical amplifiers reported were grid amplifiers [1, 2]. Subsequently, amplifier arrays employing discrete printed antennas were investigated [3-5]. In [6-7], two dimensional quasi-optical amplifiers using a dielectric slab were discussed.

The excitation of spatial amplifier arrays is an important issue. For efficient power combining, incident waves must be focused entirely on the surface of the amplifier array. Furthermore, in order to excite all the devices across the surface of the spatial amplifier uniformly, (assuming that all the devices have the same periphery), the incident power distribution across the plane of the amplifier array must be uniform. In [5], reactive field coupling from horn antennas was demonstrated as a possible method of excitation of quasi-optical amplifiers.

Advances in the theory of hard electromagnetic surfaces [8] have lead to the development of feeds with enhanced aperture efficiency. In [9], hard horn antennas were employed to construct a closed system quasi-optical amplifier at X-band. These "hard horns" have near uniform aperture field distributions, which allows for the simultaneous saturation of active devices across the amplifier's surface.

The general concept for the excitation of millimeter-wave, quasi-optical amplifiers is shown in Fig. 1. The input signal is incident upon the front side of the amplifier array via a hard horn antenna. The hard horn distributes the incident signal uniformly across the entire array. The amplified signal is then captured by the collecting hard horn antenna or directly radiated into free space [9].

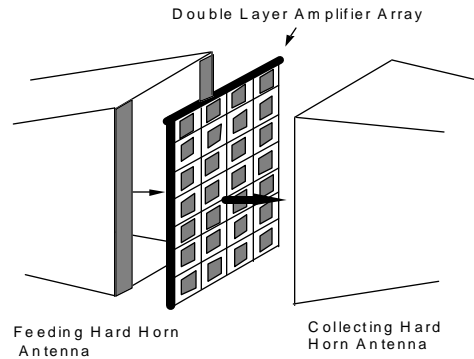


Fig.1 General concept of a closed system quasi-optical amplifier.

A pyramidal hard horn feed is shown in Fig. 2. In order to obtain a uniform aperture field distribution, two dielectric slabs with thickness  $h$  and dielectric constant  $\epsilon_r$  are placed on the E-walls of the horn. A uniform field distribution can be achieved across more than 98% of the horn aperture, if the thickness and the relative permittivity of the dielectric slabs are chosen appropriately. To achieve an optimum design, simulations of the hard horn with different dielectric constants and slab thicknesses are

necessary. In the following section, the analysis of a hard horn based on mode matching technique is described. Using this analysis, a computer program was developed to obtain the S-matrix of the horn and its aperture field distribution. This program can be employed to design optimum hard horn feeds.

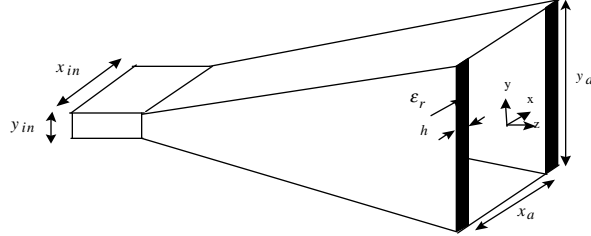


Fig. 2 A pyramidal hard horn feed

### THEORY

In this analysis the horn was approximated with a series of stair case, double plane step junctions, as shown in Figure 3. The generalized S-parameters were initially found for each step. These were then combined to get the S-matrix for the whole horn.

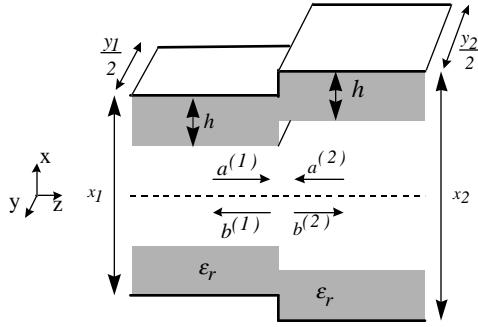


Fig. 3 A double plane step junction of a dielectric loaded rectangular waveguide.

The structure shown in Fig. 3 can support LSE<sup>x</sup> and LSM<sup>x</sup> modes. The fields are derived from the x-component of the magnetic and electric vector potentials A<sub>x</sub> and F<sub>x</sub> [10]. For the double plane step junction (Fig 4), they are given by Eqs. (1) and (2):

$$F_x = F_{xe} + F_{xo} \quad (1)$$

$$A_x = A_{xe} + A_{xo} \quad (2)$$

where:

$$F_{xe}^{(s)} = \sum_{m=0}^{\infty} \sum_{n=0}^{\infty} (a_{Fe_{mn}}^{(s)} + b_{Fe_{mn}}^{(s)}) \cdot \frac{\epsilon}{\beta_{zFe_{mn}}^{(s)}} \cdot \sqrt{Z_{Fe_{mn}}^{(s)}} T_{Fe_{mn}}^{(s)}(x, y) \quad (3)$$

$$A_{xe}^{(s)} = \sum_{m=1}^{\infty} \sum_{n=1}^{\infty} (a_{Ae_{mn}}^{(s)} + b_{Ae_{mn}}^{(s)}) \cdot \frac{\mu}{\beta_{zAe_{mn}}^{(s)}} \cdot \sqrt{Z_{Ae_{mn}}^{(s)}} T_{Ae_{mn}}^{(s)}(x, y) \quad (4)$$

The subscript *e* stands for even modes . The odd modes with subscript *o* have a similar formulation. The superscript *s*=1 denotes the fields in the waveguide on the left side of the junction whereas *s*=2 denotes the fields in the waveguide on the right side of the junction . Z<sub>A</sub> and Z<sub>F</sub> are the wave impedances for LSM<sup>x</sup> and LSE<sup>x</sup> modes, respectively.

In the above formulation, it is assumed that at the double plane discontinuity all modes are excited and that there will be incident and reflected waves for each mode. Thus, the total field is the sum of all the excited modes. T<sub>A</sub>(x,y) and T<sub>F</sub>(x,y) in the above equations are the mode functions and are normalized such that the power carried by each mode is proportional to the square amplitude of that mode [11].

The mode matching technique at the junction requires:

$$E_t^{(1)} = E_t^{(2)} \quad (\text{over area}^{(1)}) \quad (5)$$

$$H_t^{(1)} = H_t^{(2)} \quad (\text{over area}^{(2)}) \quad (6)$$

$$E_t^{(2)} = 0 \quad (\text{over (area}^{(2)} - \text{area}^{(1)}) \quad (7)$$

where the subscript *t* denotes the total transverse field at the junction.

After some manipulation, the above three equation are used to get the following:

$$\begin{bmatrix} [I] & [0] & [0] & [0] \\ [0] & [I] & [0] & [0] \\ [0] & [0] & [I] & [0] \\ [0] & [0] & [0] & [I] \end{bmatrix} H^T \begin{bmatrix} b_{Fe}^{(1)} \\ b_{Fo}^{(1)} \\ b_{Ae}^{(1)} \\ b_{Ao}^{(1)} \end{bmatrix} = \begin{bmatrix} b_{Fe}^{(1)} \\ b_{Fo}^{(1)} \\ b_{Ae}^{(1)} \\ b_{Ao}^{(1)} \end{bmatrix} \quad (8)$$

$$- H \begin{bmatrix} [I] & [0] & [0] & [0] \\ [0] & [I] & [0] & [0] \\ [0] & [0] & [I] & [0] \\ [0] & [0] & [0] & [I] \end{bmatrix} \begin{bmatrix} b_{Fe}^{(2)} \\ b_{Fo}^{(2)} \\ b_{Ae}^{(2)} \\ b_{Ao}^{(2)} \end{bmatrix} = \begin{bmatrix} b_{Fe}^{(2)} \\ b_{Fo}^{(2)} \\ b_{Ae}^{(2)} \\ b_{Ao}^{(2)} \end{bmatrix}$$

$$\begin{bmatrix} [I] & [0] & [0] & [0] \\ [0] & [I] & [0] & [0] \\ [0] & [0] & [I] & [0] \\ [0] & [0] & [0] & [I] \end{bmatrix} H^T \begin{bmatrix} a_{Fe}^{(1)} \\ a_{Fo}^{(1)} \\ a_{Ae}^{(1)} \\ a_{Ao}^{(1)} \end{bmatrix} = \begin{bmatrix} a_{Fe}^{(1)} \\ a_{Fo}^{(1)} \\ a_{Ae}^{(1)} \\ a_{Ao}^{(1)} \end{bmatrix}$$

$$H \begin{bmatrix} [-I] & [0] & [0] & [0] \\ [0] & [-I] & [0] & [0] \\ [0] & [0] & [-I] & [0] \\ [0] & [0] & [0] & [-I] \end{bmatrix} \begin{bmatrix} a_{Fe}^{(2)} \\ a_{Fo}^{(2)} \\ a_{Ae}^{(2)} \\ a_{Ao}^{(2)} \end{bmatrix} = \begin{bmatrix} a_{Fe}^{(2)} \\ a_{Fo}^{(2)} \\ a_{Ae}^{(2)} \\ a_{Ao}^{(2)} \end{bmatrix}$$

where  $[I]$  is the identity matrix and

$$H = \begin{bmatrix} [V_{FFee}] & [V_{FFoe}] & [0] \\ [V_{FFeo}] & [V_{FFoo}] & [0] \\ [0] & [V_{AAee}] & [V_{AAoe}] \\ [0] & [V_{AAeo}] & [V_{AAoo}] \end{bmatrix} \quad (9)$$

where  $V_{AA}$  and  $V_{FF}$  are matrices with their elements expressing the power coupling between the various modes.

The S-matrix of a double plane step junction dielectric-loaded waveguide is given by:

$$[S] = [B]^{-1} [A] \quad (10)$$

This is repeated at each junction. The total S-matrix of the horn is obtained by combining the matrices of all junctions following the method given in [11].

## RESULTS

A Ka-band hard horn with dimensions  $x_a \times y_a = 69 \times 53 \text{ mm}$ ,  $h=1.98 \text{ mm}$ ,  $\epsilon_r = 2.2$  and length  $l=119 \text{ mm}$ , was analyzed at a frequency of  $31 \text{ GHz}$ . The length of the horn was subdivided into 120 sections. The output field distribution magnitude and phase, are given in Figures 4a and 5a respectively. This hard horn provides a uniform field distribution within  $\pm 1 \text{ dB}$  over more than 98% of the aperture with a maximum phase error of 80 degrees with respect to the aperture center. The phase error can be corrected using a lens. Measurement of the aperture field was performed with an automated near field measurement system. Custom software was used to take the measurement and record the data. The experimental results are shown in Figures 4b and 5b. There is a general agreement between the measured and theoretical results. The differences are due to our near field measurement setup and imperfections in the placement of the dielectric slabs.

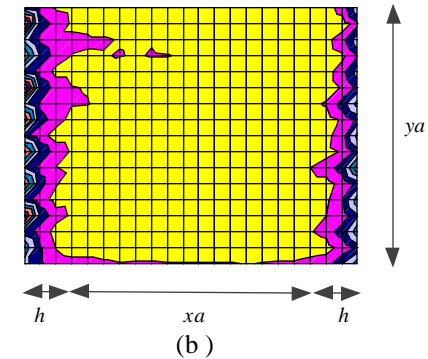
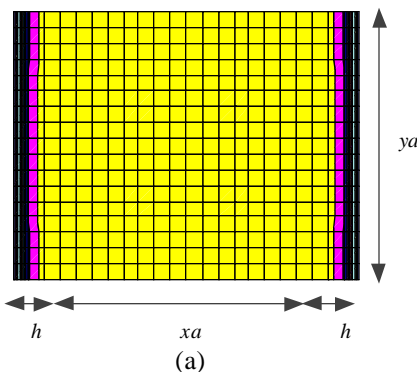


Fig.4(a)&(b): Simulated & measured magnitude distribution for the aperture field of a 31 GHz hard horn. The bright shade represents  $\pm 1 \text{ dB}$  power variation.

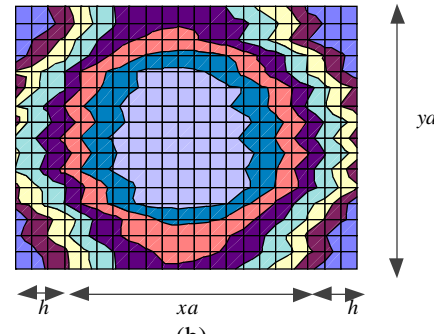
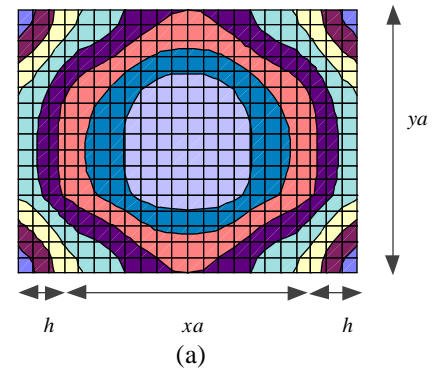


Fig.5(a)&(b): Simulated & measured phase distribution for the aperture field of a 31 GHz hard horn. Each shade of gray represents 10 degrees phase variation.

In order to study the array's power compression improvement using hard horns, a simple analysis for an  $8 \times 8$  combining amplifier array was performed. The amplifier array is assumed to be excited by a 64 way power divider. The coupling between the array elements is neglected. The power and phase distribution of the divider is dictated by measured results obtained from a  $30 \text{ GHz}$  regular and hard horn. Figure 6 shows the results for an ideal excitation (uniform amplitude and phase distribution), a regular horn, and the  $30 \text{ GHz}$  hard horn

and lens configuration. The results show that for this particular example the output power improvement is better than  $4\text{ dB}$  (at  $1\text{ dB}$  compression). This compares closely with our experimental data reported in [9].

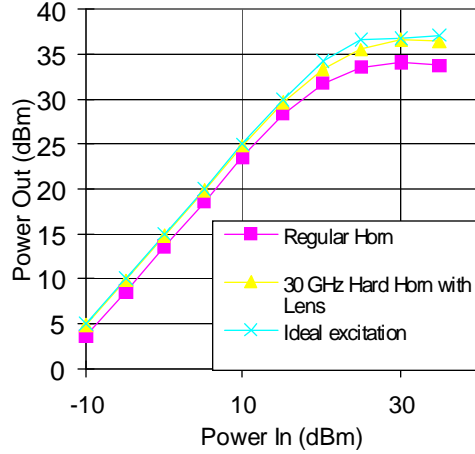


Fig. 6 Power compression curves for an 8x8 Amplifier Array

## CONCLUSION

In this paper, an analysis of hard horns for the excitation of quasi-optical amplifiers was presented. The analysis is based on the mode matching technique and results in a generalized S-matrix for the hard horn feed. This was used to develop a computationally time efficient program to help design hard horn feeds. The simulation results for a  $31\text{ GHz}$  hard horn shows close agreement with the measurement.

## ACKNOWLEDGEMENT

This project was supported by DARPA and Wright Patterson Air Force Base under Contract N66001-96-C-8628 to Lockheed-Martin Corporation.

## REFERENCES

- [1] M. Kim, J. Rosenberg, R. P. Smith, R. M. Weikle, J. B. Hacker, M. P. De Lisio, and D. B. Rutledge, "A grid amplifier," *IEEE Microwave and Guided Lett.*, vol. 1, no. 11, pp. 322-324, Nov. 1991.
- [2] M. Kim, E. A. Soverro, J. B. Hacker, M. P. De Lisio, J.-C. Chiao, S.-J. Li, D. R. Cagnon, J. J. Rosenberg, and D. B. Rutledge, "A 100-element HBT grid amplifier," *IEEE Trans. Microwave Theory Tech.*, vol. 41, no. 10, pp. 1762-1771, Oct. 1993.
- [3] T. Mader, J. Schoenberg, L. Harmon, and Z. B. Popovic, "Planar MESFET transmission wave amplifier," *Electron. Lett.*, vol. 29, no. 19, pp. 1699-1701, Sept. 1993.
- [4] H. S. Tsai, M. J. W. Rodwell, and R. A. York, "Planar amplifier array with improved bandwidth using folded slots," *IEEE Microwave and Guided Lett.*, vol. 4, no. 4, pp. 112-114, Apr. 1994.
- [5] T. Ivanov, A. Balasubramaniyan, and A. Mortazawi, "One and two stage spatial amplifiers," *IEEE Trans. Microwave Theory Tech.*, vol. 43, no. 9, pp. 2138-2143, Sept. 1995.
- [6] H. Hwang, T. W. Nuteson, M. B. Steer, J. W. Mink, J. Harvey, and A. Paoella, "A quasi-optical dielectric slab power combiner," *IEEE Microwave and Guided Lett.*, vol. 6, no. 2, pp. 73-75, Feb. 1996.
- [7] A. R. Perkins, and T. Itoh, "A 10-element active lens amplifier on a dielectric slab," *IEEE Int. Microwave Symp. '96*, Symp. Digest, vol. 2, pp. 1119-1121, Jun. 1996.
- [8] P.S. Kildal, "definition of artificially soft and hard surfaces for electromagnetic waves," *Elleewctron. Lett.*, no. 24, pp. 168-170, 1988
- [9] T. Ivanov, and A. Mortazawi, "A two-stage spatial amplifiers with hard horn feeds," *IEEE Microwave and Guided Lett.*, vol. 6, no. 2, pp. 88-90, Feb. 1996.
- [10] C.A. Balanis, "Advanced engineering electromagnetics," John Wiley & Sons, New York, 1989.
- [11] H. Patzelt, and F. Arndt, "Double-Plane Steps in Rectangular Waveguides and their Application for Transformers, Irises, and Filters," *IEEE Trans. Microwave Theory Tech.*, vol. 30, no. 5, pp. 771-776, May. 1982.